Available online at www.sciencedirect.com
ScienceDirect
International Journal of Solids and Structures 44 (2007) 387–398
INTERNATIONAL JOURNAL OF SOLIDS and STRUCTURES
www.elsevier.com/locate/ijsolstr

# Applicability of the crack-face electromagnetic boundary conditions for fracture of magnetoelectroelastic materials

Bao-Lin Wang *, Yiu-Wing Mai

*Centre for Advanced Materials Technology (CAMT), School of Aerospace, Mechanical and Mechatronic Engineering, Mechanical Engineering Building J07, University of Sydney, Sydney, NSW 2006, Australia*

Received 19 July 2005; received in revised form 1 February 2006
Available online 28 April 2006

**Abstract**

This paper discusses the different electromagnetic boundary conditions on the crack-faces in magnetoelectroelastic materials, which possess coupled piezoelectric, piezomagnetic and magnetoelectric effects. A notch of finite thickness in these materials containing air (or vacuum) is also addressed. Four ideal crack-face electromagnetic boundary condition assumptions, that is, (a) electrically and magnetically impermeable crack, (b) electrically impermeable and magnetically permeable crack, (c) electrically permeable and magnetically impermeable crack and (d) electrically and magnetically permeable crack, are investigated separately. The influence of notch thickness on the field intensity factors at notch tips and the electromagnetic field inside the notch are obtained in closed-form. The results are compared with the ideal crack solutions. Applicability of crack-face electromagnetic boundary condition assumptions is discussed.


*Keywords:* Fracture mechanics; Magnetoelectroelastic materials; Boundary conditions; Notch

## 1. Introduction

Materials possessing electro-magneto-mechanical coupling effects have found increasing applications in engineering structures, particularly in smart materials/intelligent structures. The effects of electro-magneto-mechanical coupling have been observed in single-phase materials where simultaneous electric and magnetic ordering co-exists, and in two-phase composites where the participating phases are piezo- electric and piezo-magnetic (Alshits et al., 1992; Avellaneda and Harshe, 1994; Barnet and Lothe, 1975; Benveniste, 1995; Harshe et al., 1993; Huang and Kuo, 1997; Kirchner and Alshits, 1996; Li and Dunn, 1998; Nan, 1994). In recent years, an area of increasing interest is the fracture mechanics of magnetoelectroelastic materials, which are combinations of the ferromagnetic and ferroelectric phases. One of the basic and important issues on the

* Corresponding author.
*E-mail addresses:* baolin.wang@aeromech.usyd.edu.au, wangbl2001@hotmail.com (B.-L. Wang), mai@aeromech.usyd.edu.au (Y.-W. Mai).

0020-7683/$ - see front matter © 2006 Elsevier Ltd. All rights reserved.
doi:10.1016/j.ijsolstr.2006.04.028

fracture mechanics of magnetoelectroelastic materials is the crack-face electromagnetic boundary condition. For piezoelectric materials, there are two kinds of ideal electrical boundary condition assumptions for the crack-faces, that is, electrically impermeable crack and permeable crack. Such assumptions will be applied to the magnetoelectroelastic materials to include the magnetically impermeable crack and magnetically permeable crack. Unlike in piezoelectricity, very little work has been done on the fracture characteristics of ferroelectromagnetic materials where the cracks were treated as either (a) electrically and magnetically impermeable, or (b) electrically and magnetically permeable (Liu et al., 2001; Gao et al., 2003; Wang and Mai, 2003; Wang and Mai, 2004; Tian and Gabbert, 2005; Hu and Li, 2005; Li, 2005; Gao and Noda, 2004). Recently, an elliptical cavity in a magnetoelectroelastic solid under an in-plane electro-magnetic and/or anti-plane mechanical loading was investigated (Gao et al., 2004). By reducing the cavity to a crack, the extreme cases for an impermeable crack and a permeable crack were obtained.

The main objective of this paper is to discuss the applicability of the crack-face electromagnetic boundary condition assumptions. These assumptions are: (i) electrically impermeable and magnetically permeable, (ii) electrically permeable and magnetically impermeable, (iii) fully impermeable, or (iv) fully permeable. To discuss the applicability of the crack-face electromagnetic boundary conditions, a notch of finite thickness is also studied. Only in-plane electromagnetic and mechanical loading conditions are considered. Throughout this paper, a notch is defined as a flaw in a solid with a finite gap thickness and a crack is defined as a notch with negligible gap thickness.

## 2. Foundation of two-dimensional magnetoelectroelasticity

In a fixed rectangular coordinate system, $(x_1, x_2)$, the field equations for a linear magnetoelectroelastic medium whose poling direction is along the positive $x_2$-axis can be written in the following form (Huang and Kuo, 1997):

*Constitutive equations*:

$$\begin{Bmatrix}\sigma_{11}\\ \sigma_{22}\\ \sigma_{12}\end{Bmatrix}=\begin{bmatrix}c_{11} & c_{13} & 0\\ c_{13} & c_{33} & 0\\ 0 & 0 & c_{44}\end{bmatrix}\begin{Bmatrix}\varepsilon_{11}\\ \varepsilon_{22}\\ 2\varepsilon_{12}\end{Bmatrix}-\begin{bmatrix}0 & e_{31}\\ 0 & e_{33}\\ e_{15} & 0\end{bmatrix}\begin{Bmatrix}E_1\\ E_2\end{Bmatrix}-\begin{bmatrix}0 & h_{31}\\ 0 & h_{33}\\ h_{15} & 0\end{bmatrix}\begin{Bmatrix}H_1\\ H_2\end{Bmatrix}, \tag{1a}$$

$$\begin{Bmatrix}D_1\\ D_2\end{Bmatrix}=\begin{bmatrix}0 & 0 & e_{15}\\ e_{31} & e_{33} & 0\end{bmatrix}\begin{Bmatrix}\varepsilon_{11}\\ \varepsilon_{22}\\ 2\varepsilon_{12}\end{Bmatrix}+\begin{bmatrix}\epsilon_{11} & 0\\ 0 & \epsilon_{33}\end{bmatrix}\begin{Bmatrix}E_1\\ E_2\end{Bmatrix}+\begin{bmatrix}\beta_{11} & 0\\ 0 & \beta_{33}\end{bmatrix}\begin{Bmatrix}H_1\\ H_2\end{Bmatrix}, \tag{1b}$$

$$\begin{Bmatrix}B_1\\ B_2\end{Bmatrix}=\begin{bmatrix}0 & 0 & h_{15}\\ h_{31} & h_{33} & 0\end{bmatrix}\begin{Bmatrix}\varepsilon_{11}\\ \varepsilon_{22}\\ 2\varepsilon_{12}\end{Bmatrix}+\begin{bmatrix}\beta_{11} & 0\\ 0 & \beta_{33}\end{bmatrix}\begin{Bmatrix}E_1\\ E_2\end{Bmatrix}+\begin{bmatrix}\gamma_{11} & 0\\ 0 & \gamma_{33}\end{bmatrix}\begin{Bmatrix}H_1\\ H_2\end{Bmatrix}. \tag{1c}$$

*Divergence and gradient equations:*

$$\varepsilon_{ij}=\frac{1}{2}(u_{i,j}+u_{j,i}),\quad E_i=-\phi_{,i},\quad H_i=-\varphi_{,i}. \tag{2}$$

*Equilibrium equations:*

$$\sigma_{ij,i}=0,\quad D_{i,i}=0,\quad B_{i,i}=0. \tag{3}$$

In Eqs. (1)–(3), $(i,j)=(1,2)$, and a comma denotes partial differentiation and repeated indices summation; $u_i$ is component of elastic displacement vector $\boldsymbol{u}$; $\phi$ and $\varphi$ are electric and magnetic potentials, respectively; $\sigma_{ij}$, $\varepsilon_{ij}$, $D_i$, $E_i$, $B_i$ and $H_i$ are components of stress, strain, electrical displacement, electric field, magnetic induction and magnetic field, respectively; $c_{ijkl}$, $e_{iks}$, $h_{iks}$ and $\beta_{is}$ are elastic, piezoelectric, piezomagnetic and electromagnetic constants; $\epsilon_{ij}$ and $\gamma_{ij}$ are dielectric permitivities and magnetic permeabilities.

## 3. A crack in magnetoelectroelastic media

Fig. 1 shows a crack of length $2a$ lies along the $x_1$-axis. The magnetoelectroelastic medium is loaded by a remote uniform stress $\sigma_{22} = \sigma_0$, a uniform electric displacement $D_2 = D_0$, and a uniform magnetic induction $B_2 = B_0$. Since the medium inside the crack (usually air or vacuum) allows some penetration of the electromagnetic field, the normal components of the electric displacement and the magnetic induction on the crack-faces may not be zero and they are denoted as $d_0$ and $b_0$, respectively.

If we consider an asymptotic problem, then the equivalent crack-face magnetoelectroelastic loads are $-\boldsymbol{t}_0(x_1) = -(\sigma_0, D_0 - d_0, B_0 - b_0)^{\mathrm{T}}$. Thus, on the $y = 0$ plane, we have the mixed-mode boundary conditions:

$$\sigma_{22}(x,0) = -\sigma_0, \quad D_2(x,0) = -D_0 + d_0, \quad B_2(x,0) = -B_0 + b_0, \quad \text{for } |x| < a, \tag{4}$$

$$u_2(x,0) = 0, \quad \phi(x,0) = 0, \quad \varphi(x,0) = 0, \quad \text{for } |x| \geqslant a, \tag{5}$$

$$\sigma_{12}(x,0) = 0, \quad \text{for } |x| \geqslant 0. \tag{6}$$

Using the following notation:

$$\boldsymbol{v} = (u_2, \phi, \varphi)^{\mathrm{T}}, \tag{7}$$

then the solution for the crack problem can be obtained as follows (Wang and Mai, 2003):

(a) The jumps of normal displacement, electric potential and magnetic potential across the crack-faces are obtained from:

$$\Delta\boldsymbol{v} = (\Delta u_2, \Delta\phi, \Delta\varphi)^{\mathrm{T}} = 4\sqrt{a^2 - x_1^2}[\boldsymbol{\Lambda}]\boldsymbol{t}_0, \tag{8}$$

where $[\boldsymbol{\Lambda}]$ is a $3 \times 3$ matrix.

(b) The field intensity factors are:

$$\boldsymbol{K} = \{K_{\mathrm{I}}, K_{\mathrm{D}}, K_{\mathrm{B}}\}^{\mathrm{T}} = \boldsymbol{t}_0\sqrt{\pi a} = (\sigma_0, D_0 - d_0, B_0 - b_0)^{\mathrm{T}}\sqrt{\pi a}, \tag{9}$$

where $K_{\mathrm{I}}$ is traditional stress intensity factor, $K_{\mathrm{D}}$ and $K_{\mathrm{B}}$ are, respectively, electric displacement intensity factor and magnetic induction intensity factor. The full field solution near the crack-tip has been given in terms of the field intensity factors by Wang and Mai (2003).

(c) The energy release rate $G$ at the crack-tip is obtained from the following integral:

$$G = \frac{1}{2}\lim_{\delta\to 0}\frac{1}{\delta}\int_0^{\delta}(\sigma_{22}(r+a,0)\Delta u_2(r+a-\delta) + D_2(r+a,0)\Delta\phi(r+a-\delta) + B_2(r+a,0)\Delta\varphi(r+a-\delta))\,\mathrm{d}r \tag{10}$$

and the result becomes:

$$G = (K_{\mathrm{I}}, K_{\mathrm{D}}, K_{\mathrm{B}})[\boldsymbol{\Lambda}](K_{\mathrm{I}}, K_{\mathrm{D}}, K_{\mathrm{B}})^{\mathrm{T}}. \tag{11}$$

Since the load vector $\boldsymbol{t}_0$ contains unknown parameters $d_0$ and $b_0$, additional assumptions are needed to obtain the solution to the problem (See Sections 4 and 5 for details). Eq. (9) clearly shows that the stress intensity factor depends only on the applied mechanical loads. However, the electric displacement and magnetic induction intensity factors are dependent on the material constants since the unknown crack-face electric displacement and magnetic induction depend on the material properties. (Details are given in Sections 4 and 5).

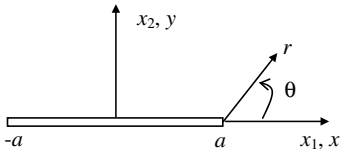


Fig. 1. A straight crack in magnetoelectroelastic media.

## 4. Solutions based on ideal crack-face boundary conditions

For piezoelectric materials, there are two kinds of ideal electric boundary condition assumptions for the crack-faces, that is, electrically impermeable crack and electrically permeable crack (Zhang et al., 2002, 2001). Such assumptions can be applied to magnetoelectroelastic media to include: (a) electrically impermeable crack so that the normal electric displacement on the crack-faces is zero; (b) electrically permeable crack, that is, the electric potential jump across the crack is assumed zero; (c) magnetically impermeable crack such that the normal magnetic induction on the crack-faces is zero; and (d) magnetically permeable crack so that the magnetic potential jump across the crack is zero.

In most practical applications, however, the crack-face boundary conditions can be treated as: (i) electrically impermeable and magnetically permeable, (ii) electrically permeable and magnetically impermeable, (iii) fully impermeable, or (iv) fully permeable. In each of these cases (i)–(iv), we can obtain the full field solutions of the problem. We discuss these separately below.

### 4.1. Electrically and magnetically impermeable crack

In this case, the normal electric displacement and magnetic induction on the crack-faces are zero. Thus,

$$d_0 = 0, \quad b_0 = 0. \tag{12}$$

### 4.2. Electrically and magnetically permeable crack

Here, the electric and magnetic potential jumps across the crack-faces are zero:

$$\Delta\phi = 0, \quad \Delta\varphi = 0. \tag{13}$$

So, from Eq. (8),

$$\Lambda_{21}\sigma_0 + \Lambda_{22}(D_0 - d_0) + \Lambda_{23}(B_0 - b_0) = 0, \tag{14a}$$

$$\Lambda_{31}\sigma_0 + \Lambda_{32}(D_0 - d_0) + \Lambda_{33}(B_0 - b_0) = 0. \tag{14b}$$

Eqs. (14) can be used to solve for $d_0$ and $b_0$. From Eqs. (9) and (11), it is apparent that the near tip solutions depend on $\sigma_0$, $D_0 - d_0$ and $B_0 - b_0$. From Eqs. (14), we know that $D_0 - d_0$ and $B_0 - b_0$ are determined by the applied stress $\sigma_0$. Therefore, solutions for the fully permeable crack are independent of applied electric displacement and magnetic induction.

### 4.3. Electrically impermeable and magnetically permeable crack

In this case, the normal electric displacement on the crack-faces and the magnetic potential jump across the crack are zero. Therefore, we have

$$d_0 = 0, \quad \Lambda_{31}\sigma_0 + \Lambda_{32}D_0 + \Lambda_{33}(B_0 - b_0) = 0. \tag{15}$$

Eq. (15) can be used to solve for $b_0$. It can be seen that $B_0 - b_0$ is determined by the applied stress $\sigma_0$ and electric displacement $D_0$. Hence, the solutions for the electrically impermeable and magnetically permeable crack are independent of applied magnetic induction.

### 4.4. Electrically permeable and magnetically impermeable crack

Now, the normal magnetic induction on the crack-faces and the electric potential jump across the crack – faces are both zero such that:

$$\Lambda_{21}\sigma_0 + \Lambda_{22}(D_0 - d_0) + \Lambda_{23}B_0 = 0, \quad b_0 = 0. \tag{16}$$

Eq. (16) can be used to solve for $d_0$. Clearly, $D_0 - d_0$ is determined by applied stress $\sigma_0$ and magnetic induction $B_0$. Therefore, solutions for the electrically permeable and magnetically impermeable crack are independent of the remote applied electric displacement.

In each case of (i)–(iv), the normal components of electric displacement and magnetic induction on the crack-faces can be solved. Once they are determined, the vector $\boldsymbol{t}_0$ is known and the field intensity factors and the energy release rate can be obtained from Section 3. The near crack-tip expressions for the magneto-electroelastic fields have already been provided by Wang and Mai (2003).

## 5. The accuracy of the ideal crack surface boundary conditions

In Section 4, we consider a flaw in the magnetoelectroelastic media as a cleavage crack of zero gap thickness. Both impermeable and permeable crack-face electric and magnetic boundary conditions are studied. Of these extreme cases, the permeable crack assumption simply treats the crack as electrically and magnetically conductive, while the impermeable assumption considers the crack as electrically and magnetically insulated. In engineering practices, however, flaws in a medium are not like cleavage cracks of zero gap width, but rather like notches with a finite (but very small) width (see Fig. 2). Strictly, even if the electric and magnetic permittivities of air or vacuum inside the crack are small, the fluxes of an electric and magnetic fields through the crack should not be zero. Hence, it is more reasonable to consider the electric and magnetic fields inside the notch and the electric and magnetic potential jumps across the notch simultaneously.

Suppose the notch profile $\delta(x)$ is sufficiently small, except near the notch tips, the gradient of notch opening along the notch is small. Along the $x_2$-axis the normal components of the electric field $E_0$ and the electric displacement $d_0$ inside the notch can be written in terms of the electric and magnetic potential jumps $\Delta\phi$ as (McMeeking, 1999):

$$E_0(x) = -\frac{\Delta\phi(x)}{2\delta(x)}, \quad d_0(x) = -\epsilon_0\frac{\Delta\phi(x)}{2\delta(x)}. \tag{17}$$

Analogously, the normal components of the magnetic field $H_0$ and the magnetic induction $b_0$ inside the notch are:

$$H_0(x) = -\frac{\Delta\varphi(x)}{2\delta(x)}, \quad b_0(x) = -\gamma_0\frac{\Delta\varphi(x)}{2\delta(x)}. \tag{18}$$

In Eqs. (17) and (18), $\epsilon_0$ and $\gamma_0$ are dielectric constant and magnetic permeability of the medium inside the notch, which is usually air or vacuum.

In the following, we consider an elliptic profile of the notch, that is,

$$\delta(x) = \sqrt{a^2 - x_1^2}\left(\frac{\delta_0}{a}\right), \tag{19}$$

where $\delta_0$ is notch half-thickness at $x_1 = 0$ (see Fig. 2). Since the notch profile $\delta(x)$ is sufficiently small, the crack solution in Section 3 can still be approximately applied to the notch problem. Therefore, Eq. (8) can be substituted into Eqs. (17) and (18) through Eq. (19). This leads to:

$$d_0 = -2\frac{a}{\delta_0}\epsilon_0[\Lambda_{21}\sigma_0 + \Lambda_{22}(D_0 - d_0) + \Lambda_{23}(B_0 - b_0)], \tag{20a}$$

$$b_0 = -2\frac{a}{\delta_0}\gamma_0[\Lambda_{31}\sigma_0 + \Lambda_{32}(D_0 - d_0) + \Lambda_{33}(B_0 - b_0)]. \tag{20b}$$

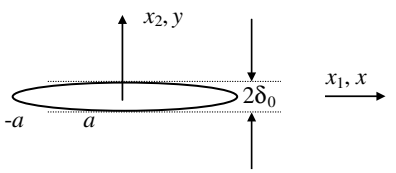


Fig. 2. A notch of finite thickness.

Due to the existence of the coupling coefficients $\Lambda_{23}$ and $\Lambda_{32}$ ($\Lambda_{23} = \Lambda_{32}$) between the electric and magnetic fields, the analytical and closed-form expressions for the electric displacement $d_0$ and magnetic induction $b_0$ inside the notch are not available. However, $d_0$ and $b_0$ can be easily solved from the linear algebraic Eqs. (20). Once $d_0$ and $b_0$ are known, the near-tip field intensity factors and the energy release rate can be obtained from the solution given in Section 3. It can be seen from Eqs. (20), if both $\epsilon_0$ and $\gamma_0$ are zero (or the notch gap $\delta_0$ is infinite), the fully impermeable crack solutions are recovered. Conversely, if $\epsilon_0$ and $\gamma_0$ are infinite (or the notch gap $\delta_0$ is zero), the results are reduced to the fully permeable crack solution.

## 6. Applications

Numerical results are given in this Section for a crack and a notch in a $BaTiO_3$–$CoFe_2O_4$ composite, which is a magnetoelectroelastic material, subjected independently to a uniform tension, a uniform electric displacement, and a uniform magnetic induction, remote from the crack/notch. Since the system is linear, the solutions for any combination of electro-magneto-mechanical loads can be determined directly from these independent solutions.

### 6.1. Material properties

The non-zero material constants for $BaTiO_3$ and $CoFe_2O_4$ are given in Table 1 (Huang, 1998). The medium inside the notch is air (or vacuum) whose electric permeability and magnetic permeability are, respectively, $\epsilon_0 = 0.0885 \times 10^{-10}$ N/V$^2$ and $\gamma^0 = 4\pi \times 10^{-7}$ N/A$^2$.

It should be noted that the value of $\gamma_{11}$ for $CoFe_2O_4$ used in a number of papers is negative (e.g., Huang and Kuo, 1997; Hu and Li, 2005; Aboudi, 2001; Lage et al., 2004; Chen et al., 2002). Sih et al. also used a negative value of $\gamma_{11}(= -59 \times 10^{-5}$ Ns$^2$/C$^2$) for $CoFe_2O_4$. (See Sih and Song (2003), Spyropoulos et al. (2003) and references cited therein). However, they reversed the sign of $\gamma_{11}$ for $CoFe_2O_4$ to positive when they determined the overall properties of the $BaTiO_3$–$CoFe_2O_4$ composites using the rule of mixtures.

For stable materials, the magnetic permeabilities $\gamma_{ij}$, like elastic constants and dielectric permeabilities, should be positive definite, that is, $\gamma_{ij}H_iH_j > 0$ for any non-zero real vector $\boldsymbol{H}$. This means that the material constants $\gamma_{11}$, $\gamma_{22}$ and $\gamma_{33}$ should be greater than zero and negative material constants are not physically

Table 1
Non-zero properties for $BaTiO_3$ and $CoFe_2O_4$ single-phase materials and $BaTiO_3$–$CoFe_2O_4$ composite

| | $BaTiO_3$ | $CoFe_2O_4$ | $BaTiO_3$–$CoFe_2O_4$ composite ([b]) |
|---|---|---|---|
| $c_{11}$ ($10^{10}$N/m$^2$) | 16.6 | 28.6 | 22.6 |
| $c_{13}$ ($10^{10}$N/m$^2$) | 7.8 | 17.05 | 12.4 |
| $c_{33}$ ($10^{10}$N/m$^2$) | 16.2 | 26.95 | 21.6 |
| $c_{44}$ ($10^{10}$N/m$^2$) | 4.3 | 4.53 | 4.4 |
| $c_{12}$ ($10^{10}$N/m$^2$) | 7.7 | 17.3 | 12.5 |
| $e_{31}$ (C/m$^2$) | −4.4 | | −2.2 |
| $e_{33}$ (C/m$^2$) | 18.6 | | 9.3 |
| $e_{15}$ (C/m$^2$) | 11.6 | | 5.8 |
| $\epsilon_{11}$ [$10^{-10}$ C$^2$/(Nm$^2$)] | 112 | 0.8 | 56.4 |
| $\epsilon_{33}$ [$10^{-10}$ C$^2$/(Nm$^2$)] | 126 | 0.93 | 63.5 |
| $\gamma_{11}$ ($10^{-10}$ Ns$^2$/C$^2$) | 50,000 | ([a]) | 810,000 |
| $\gamma_{33}$($10^{-10}$ Ns$^2$/C$^2$) | 100,000 | 1,570,000 | 835,000 |
| $h_{31}$ [N/(Am)] | | 580.3 | 290.2 |
| $h_{33}$ [N/(Am)] | | 699.7 | 350 |
| $h_{15}$ [N/(Am)] | | 550 | 275 |

Material properties for $BaTiO_3$ and $CoFe_2O_4$ are taken from Huang (1998).

[a] Since a negative value of $\gamma_{11}$ is not admissible (see comments in Section 6.1) and a reasonable positive value of $\gamma_{11}$ for $CoFe_2O_4$ is unavailable in the literature, in this work, the value $\gamma_{11} = \gamma_{33} = 125\gamma^0$ for $CoFe_2O_4$ is assumed.

[b] The properties of $BaTiO_3$–$CoFe_2O_4$ composite are obtained by averaging the properties of single-phase $BaTiO_3$ and $CoFe_2O_4$ materials. (This implies that the $BaTiO_3$ to $CoFe_2O_4$ ratio in the composite is roughly 50:50).

admissible. To our understanding, if $\gamma_{11}$ is negative, the system becomes mathematically ill-posed. Only Gao et al. (2004) uses a positive value for $\gamma_{11}$ which is $59\times10^{-5}$ $Ns^2/C^2$.

In Sections 6.2–6.4, we assume the poling direction of the magnetoelectroelastic composite to coincide with the positive $y$-axis and the applied far-field in-plane magnetoelectromechanical loads are: $\sigma_{yy}=\sigma_0$, $D_y=D_0$ and $B_y=B_0$. Using the properties of $BaTiO_3$–$CoFe_2O_4$ composite in the last column of Table 1, the material property matrix $[\Lambda]$ is obtained as:

$$[\Lambda]=\begin{bmatrix} 6.363\times10^{-12} & 0.005536 & 1.428\times10^{-5} \\ 0.005536 & -7.417\times10^{7} & 2.087\times10^{4} \\ 1.428\times10^{-5} & 2.087\times10^{4} & -6.011\times10^{3} \end{bmatrix}. \tag{21}$$

### 6.2. Solutions for ideal crack-face with different electromagnetic boundary condition assumptions

As discussed above, the stress intensity factor $K_{\mathrm{I}}$ relies only on the applied mechanical load. The notch thickness and the crack-face electromagnetic boundary condition assumption have no effect on $K_{\mathrm{I}}$. For the material property matrix $[\Lambda]$ given in Eq. (21), the electric displacement and magnetic induction intensity factors for ideal crack-face boundary conditions are obtained below:

(i) Fully impermeable crack assumption:

$$d_0=0,\quad b_0=0, \tag{22a}$$

$$K_{\mathrm{D}}=D_0\sqrt{\pi a},\quad K_{\mathrm{B}}=B_0\sqrt{\pi a}. \tag{22b}$$

(ii) Fully permeable crack assumption: Using Eqs. (14) and the material property matrix Eq. (21), the electromagnetic field and the field intensity factors become:

$$d_0=D_0-0.7538\times10^{-10}\sigma_0,\quad b_0=B_0-26.38\times10^{-10}\sigma_0, \tag{23a}$$

$$K_{\mathrm{D}}=0.7538\times10^{-10}\sigma_0\sqrt{\pi a},\quad K_{\mathrm{B}}=26.38\times10^{-10}\sigma_0\sqrt{\pi a}. \tag{23b}$$

(iii) Electrically impermeable and magnetically permeable crack assumption:

$$d_0=0,\quad b_0=B_0-23.76\times10^{-10}\sigma_0-3.472D_0, \tag{24a}$$

$$K_{\mathrm{D}}=D_0\sqrt{\pi a},\quad K_{\mathrm{B}}=(23.76\times\ 10^{-10}\sigma_0+3.472D_0)\sqrt{\pi a}. \tag{24b}$$

(iv) Electrically permeable and magnetically impermeable crack assumption:

$$d_0=D_0-0.7464\times10^{-10}\sigma_0-2.813\times10^{-4}B_0,\quad b_0=0, \tag{25a}$$

$$K_{\mathrm{D}}=(0.7464\times10^{-10}\sigma_0+2.813\times10^{-4}B_0)\sqrt{\pi a},\quad K_{\mathrm{B}}=B_0\sqrt{\pi a}. \tag{25b}$$

### 6.3. Notch solution

Now consider the problem in which the notch has a finite thickness rather than a slit crack. The electric and magnetic fields inside the notch are calculated from Eqs. (20) for specific values of the notch length to width ratio $a/\delta_0$. The expressions can be written in closed-form, but unlike Eqs. (22)–(25) they are functions of the notch thickness to length ratio. Hence, the results are presented only in graphical forms and reported independently below for the application of an applied stress, an electric displacement and a magnetic induction.

#### 6.3.1. Applied stress $\sigma_0$

The dependence of the electric displacement and the magnetic induction inside the notch, together with the electric displacement intensity factor and the magnetic induction intensity factor at the notch tip, on the notch thickness to length ratio is plotted in Fig. 3, for an applied stress $\sigma_0$. The gap thickness is shown to have a major influence on the electromagnetic fields inside the notch and the electromagnetic field intensities at the

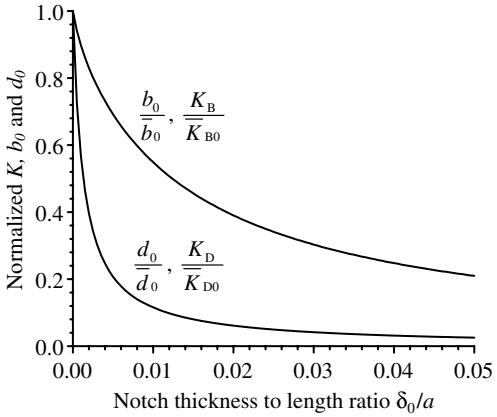


Fig. 3. Electric displacement and magnetic induction on the notch surfaces, and electric displacement and magnetic induction intensity factors at the notch tips for an applied stress $\sigma_0$ ($\overline{d}_0 = -0.7538 \times 10^{-10}\sigma_0$ and $\overline{b}_0 = -26.38 \times 10^{-10}\sigma_0$) are, respectively, electric displacement and magnetic induction inside the notch for the full permeable crack assumption (Eq. (23a)); $\overline{K}_{D0} = 0.7538 \times 10^{-10}\sigma_0\sqrt{\pi a}$ and $\overline{K}_{B0} = 26.38 \times 10^{-10}\sigma_0\sqrt{\pi a}$ are, respectively, electric displacement intensity factor and magnetic induction intensity factor for the full permeable crack assumption (Eq. (23b). The negative values of $\overline{d}_0$ and $\overline{b}_0$ imply that a tensile stress will produce a negative electric displacement and a negative magnetic induction inside the notch.

notch tip. The results decrease from the originally permeable crack solutions with $\delta_0/a$ to the impermeable crack solutions. The idealization of the fully permeable assumption is only reasonable for very small notch aspect ratios. If $\delta_0/a$ is zero such that the upper and lower surfaces of the notch are in contact, the results reduce to the fully permeable crack solutions. The electric displacement inside the notch for fully impermeable assumption is retained (with relative error less than 2.5%) for a notch aspect ratio of 0.05 or greater. It seems that the notch can be treated as an electrically impermeable crack. However, the magnetic induction inside the notch for the fully impermeable assumption is still not retained for a notch aspect ratio of 0.1 or greater (with relative error greater than 10%). Neither the impermeable crack assumption nor the permeable crack assumption can give a reasonable solution for the magnetic induction inside the notch $b_0$. Therefore, knowledge of notch width to length ratio is essential for obtaining the correct $b_0$ and $K_B$.

### 6.3.2. Applied electric displacement $D_0$

Fig. 4 shows the normal components of the electric displacement and magnetic induction vectors inside the notch, and the electric displacement intensity factor and the magnetic induction intensity factor at the notch tip for an electric displacement $D_0$. It can be seen that the normal electric displacement inside the notch $d_0$ decreases monotonously from the permeable crack solution with $\delta_0/a$ to the impermeable crack solution. Variation of $b_0$ and $K_B$ with $\delta_0/a$ are more complicated than those of $d_0$ and $K_D$ with $\delta_0/a$. It can be seen from Fig. 4 that, as $\delta_0/a$ increases, $b_0$ increases from the originally fully permeable crack solution, to a peak value, and then decreases to the fully impermeable crack solution. From Eqs. (22a) and (23a) we know that the magnetic induction $b_0$ inside the notch is zero either for the fully impermeable crack assumption or for the fully permeable crack assumption. (Note that the only applied load is $D_0$, and $B_0$ and $\sigma_0$ are zero). Hence, neither the fully electrically impermeable assumption nor the fully permeable crack assumption can give a reasonable prediction for the magnetic induction inside the notch.

### 6.3.3. Applied magnetic induction $B_0$

Fig. 5 shows the variation of the electric displacement and the magnetic induction inside the notch, and the electric displacement intensity factor and the magnetic induction intensity factor at the notch tip, with different notch thickness to length ratios for an applied magnetic induction $B_0$. Here, the normal magnetic induction inside the notch $b_0$ decreases monotonously from the originally permeable crack solution with $\delta_0/a$ to the impermeable crack solution. Unless the crack is extremely flat (that is, for $\delta_0/a$ smaller than 0.005), the idealization of a magnetically permeable assumption is not reasonable. In contrast, the magnetically impermeable

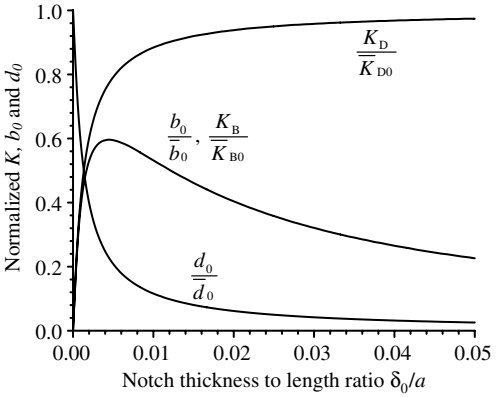


Fig. 4. Electric displacement and magnetic induction on the notch surfaces, and electric displacement and magnetic induction intensity factors at the notch tips for an applied electric displacement $D_0$ ($\overline{d}_0 = D_0$) is electric displacement inside the notch for the electrically permeable crack assumption; $\overline{b}_0 = -3.472D_0$ is magnetic induction inside the notch for the electrically impermeable and magnetically permeable crack assumption (Eq. (24a); $\overline{K}_{D0} = D_0\sqrt{\pi a}$ is electric displacement intensity factor and $\overline{K}_{B0} = 3.472D_0\sqrt{\pi a}$ is magnetic induction intensity factor for the electrically impermeable and magnetically permeable crack assumption (Eq. (24b). The negative value of $\overline{b}_0$ implies that a positive electric displacement will produce a negative magnetic induction inside the notch.

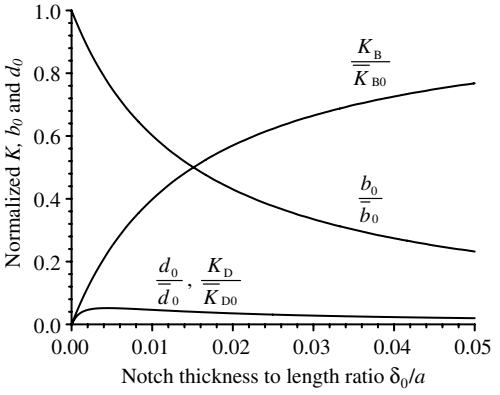


Fig. 5. Electric displacement and magnetic induction on the notch surfaces, and electric displacement and magnetic induction intensity factors at the notch tips for an applied magnetic induction $B_0$ ($\overline{d}_0 = -2.813 \times 10^{-4}B_0$) is electric displacement inside the notch for the electrically permeable and magnetically impermeable crack assumption (Eq. (25a); $\overline{b}_0 = B_0$ is magnetic induction inside the notch for the magnetically permeable crack assumption; $\overline{K}_{D0} = 2.813 \times 10^{-4}B_0\sqrt{\pi a}$ and $\overline{K}_{B0} = B_0\sqrt{\pi a}$ are, respectively, electric displacement intensity factor and magnetic induction intensity factor for the electrically permeable and magnetically impermeable crack assumption (Eq. (25b). The negative value of $\overline{d}_0$ implies that a positive magnetic induction will produce a negative electric displacement inside the notch.

assumption is still not retained for a notch aspect ratio of 0.1 or greater (with relative error greater than 10%). These results again confirm that neither magnetically impermeable crack assumption nor magnetically permeable crack assumption can provide a correct prediction for the magnetic field inside the crack.

Variation of $d_0$ and $K_D$ with $\delta_0/a$ are more complicated than those of $b_0$ and $K_B$ with $\delta_0/a$. From Eqs. (22a) and (23a), we know that the electric displacement $d_0$ inside the notch is zero either for the fully impermeable crack or the fully permeable crack. (Here, the only applied load is $B_0$, both $D_0$ and $\sigma_0$ are zero). For finite vales of $\delta_0/a$, because of the magnetoelectric coupling, the electric displacement inside the notch does not vanish. It can be shown from Fig. 5 that as $\delta_0/a$ increases, $d_0$ increases from the originally fully permeable crack solution, to a peak value, and then decreases to the fully impermeable crack solution. It seems that the electric displacement inside the notch is not significant for an applied magnetic induction.

### 6.4. Energy release rate

Energy release rate $G$ is an important fracture mechanics parameter. Here, we show the variation of $G$ with notch thickness to length ratio $\delta_0/a$. Once again, the applied electro-magneto-mechanical loads $(\sigma_0, D_0, B_0)$ are considered independently. First, $G$ is obtained in closed-form for the fully impermeable crack assumption and the fully permeable crack assumption from Eqs. (11), (22b) and (23b), with the material property matrix $[\Lambda]$ in Eq. (21):

(i) Fully impermeable crack assumption:

$$G = \pi a(6.363 \times 10^{-12}\sigma_0^2 - 7.417 \times 10^{7}D_0^2 - 6.011 \times 10^{3}B_0^2 + 0.01107\sigma_0 D_0 + 2.856 \times 10^{-5}\sigma_0 B_0 + 4.173 \times 10^{4}D_0 B_0). \tag{26a}$$

(ii) Fully permeable crack assumption:

$$G = \pi a(6.820 \times 10^{-12}\sigma_0^2). \tag{26b}$$

Three observations can be made from Eqs. (26). The first is that for the fully impermeable crack the energy release rate $G$ is always negative for a pure applied electric displacement or magnetic induction. The second is that, for the fully permeable crack, $G$ is always positive, which does not depend on the electric load $D_0$ and the magnetic load $B_0$. The third is that, even in the case of pure mechanical load, the energy release rates for the fully impermeable crack and the fully permeable crack are different. ($G$ for the fully permeable crack is about 7% higher than that for the impermeable crack).

Similar to the field intensity factors, the energy release rate for the notch is a function of the notch thickness to length ratio. Again, the results have to be presented in graphical forms. In Fig. 6, the values of the energy release rate $G$ for independent stress, electric displacement and magnetic induction applied on the medium are plotted as functions of notch thickness to length ratio $\delta_0/a$. Results are normalized by the fully impermeable crack solutions. $G$ is always negative for pure applied electric displacement or pure magnetic induction. The effect of $\delta_0/a$, for the pure applied stress case, is less important than for those cases for pure applied electric displacement and magnetic induction. For the electromagnetic loads, the effect of $\delta_0/a$, for applied magnetic induction, is much more pronounced than for applied electric displacement. It is interesting to note that for a notch thickness to length ratio $\delta_0/a$=0.05, the energy release rate for a pure electric displacement load ($D_0$) is $G = -7.040 \times 10^{7}\pi a D_0^2$, which is almost 95% of the impermeable crack solution (which is $\overline{G}_{D0} = -7.417\times$

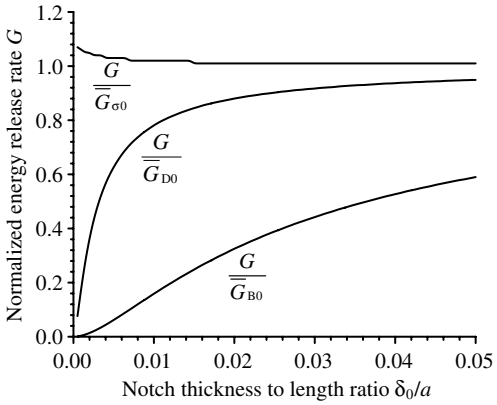


Fig. 6. Energy release rate for independent stress, electric displacement and magnetic induction applied on the medium ($\overline{G}_{\sigma 0} = 6.363 \times 10^{-12}\pi a\sigma_0^2$, $\overline{G}_{D0} = -7.417 \times 10^{7}\pi a D_0^2$, and $\overline{G}_{B0} = -6.011 \times 10^{3}\pi a B_0^2$) are the values of $G$ for pure stress $\sigma_0$, pure electric displacement $D_0$, and pure magnetic induction $B_0$, for the fully impermeable crack (Eq. (26a). The negative values of $\overline{G}_{D0}$ and $\overline{G}_{B0}$ imply that a positive value electric displacement or magnetic induction will produce a negative energy release rate.

$10^7\pi aD_0^2$). However, for the same notch thickness to length ratio ($\delta_0/a$=0.05), $G$ for a pure magnetic induction load ($B_0$) is: $G=-3.545\times10^3\pi aB_0^2$, a value just 59% of the impermeable crack solution (i.e. solution for $\delta_0/a=\infty$), which is: $\overline{G}_{B0}=-6.011\times10^3\pi aB_0^2$. Even for a larger notch thickness to length ratio, say $\delta_0/a$=0.1, $G$ for a pure electric displacement load ($D_0$) is only 3% less than the impermeable crack solution, but $G$ for a pure magnetic induction load ($B_0$) is still 25% less than the impermeable crack solution. These results indicate that, if there is an applied magnetic induction on the medium, the solution based on the impermeable crack assumption is inaccurate; and that when there is an applied electric displacement, the impermeable crack solution is quite reliable. It follows that the effect of magnetic permeability of air (or vacuum) inside the notch is more significant than the electric permeability. An explanation can be found from the material data in Table 1, which shows that the electric permeability of the magnetoelectroelastic composite medium is almost three orders larger than the electric permeability of air (vacuum). In contrast, the composite medium magnetic permeability is only two orders the magnetic permeability of air (or vacuum). Therefore, neglecting the magnetic permeability of the medium inside the notch will have more significant consequence on $G$ than neglecting the electric permeability.

## 7. Concluding remarks

The following conclusions can be made based on the results obtained in the previous sections:

(a) The stress intensity factor does not depend on the crack-face electric and magnetic boundary condition assumptions.
(b) The electric and magnetic permeabilities of air or vacuum inside the crack cannot be ignored. The effect of finite thickness of a notch or width of a crack in a realistic structure must be assessed. That is, knowledge of the notch thickness to length ratio is essential to obtaining the correct magnetic induction inside the notch $b_0$ and magnetic induction intensity factor at the notch tip $K_B$. Neither the magnetically impermeable crack assumption nor magnetically permeable crack assumption can give reasonable predictions for $b_0$ and $K_B$.
(c) Notch/crack tip energy release rate $G$ is dependent on the electromagnetic boundary conditions on the notch/crack-faces. The notch thickness to length ratio has a strong influence on $G$. The ideal crack electromagnetic boundary conditions cannot give reasonable solutions for real notches in real electro-magnetic materials, unless the notch thickness to length ratio is considered.

In closing, it must be emphasized that basic discrepancy exists in the field singularity for a crack and a notch. For an elliptic hole, unlike a crack, the field has no singularity. Therefore, it should be noted that:

(1) the field intensity factors presented in Section 5 are only valid for very flat notches (that is, the notch thickness to length ratio $\delta/a$ is very small), and
(2) the electromagnetomechanical fields obtained from Section 5 are valid at positions not very near the notch-tip.

Further, there is a substantial experimental and theoretical literature for piezoelectric materials about the applicability of permeable or impermeable boundary conditions. Also, experimental results are available about the permittivity inside a crack of a piezoelectric material. However, we cannot find any such data in the open literature for magnetoelctromechanical fracture. But comparisons with experimental results are critical to assess the most appropriate boundary conditions. Work is underway in our laboratory and test results will be published in future.

The final point that needs to be addressed is that, in this paper, the values of a magnetoelectroelastic composite material are taken as if it would be a perfect continuum. Typically, this material has grain sizes of more than 1 μm which must be compared with the crack opening displacements (COD). At the crack tip COD's are typically below 100 nm and the material is locally inhomogeneous. This means that only far behind the crack-tip might it be treated as a continuum. Near the crack-tip the material property values are best approximates.

## Acknowledgements

We are grateful to the Australian Research Council (ARC) for the financial support of this work through the Discovery Projects (#DP0346037 and #DP0665856). BLW and YWM are, respectively, Australian Research Fellow and Australian Federation Fellow supported by the ARC and tenable at the CAMT of the University of Sydney. Comments from the two anonymous reviewers on the original manuscript are especially useful for the improvement of presentation and quality of the final paper.

## References

Aboudi, J., 2001. Smart Mater. Struct. 10, 867.
Alshits, I., Darinskii, A.N., Lothe, J., 1992. Wave Motion 16, 265.
Avellaneda, M., Harshe, G., 1994. J. Intell. Mater. Syst. Struct. 5, 501.
Barnet, D.M., Lothe, J., 1975. Phys. Status Solidi B – Basic Res. 67, 105.
Benveniste, Y., 1995. Phys. Rev. B. 51, 424.
Chen, Z.R., Yu, S.W., Lu, M., Ye, L., 2002. Compos. Struct. 57, 177.
Gao, C.F., Noda, N., 2004. Int. J. Eng. Sci. 42, 1347.
Gao, C.F., Kessler, H., Balke, H., 2003. Int. J. Eng. Sci. 41, 969.
Gao, C.F., Tong, P., Zhang, T.Y., 2004. Int. J. Solids Struct. 41, 6613.
Harshe, G., Dougherty, J.P., Newnham, R.E., 1993. Int. J. Appl. Electromagn. Mater. 4, 145.
Hu, K.Q., Li, G.Q., 2005. Int. J. Solids Struct. 42, 2823.
Huang, J.H., 1998. J. Appl. Phys. 83, 5364.
Huang, J.H., Kuo, W.S., 1997. J. Appl. Phys. 81, 1378.
Kirchner, H.O.K., Alshits, V.I., 1996. Philos. Mag. A. 74, 861.
Lage, R.G., Mota, S.C.M., Mota, C.A.S., Reddy, J.N., 2004. Comput. Struct. 82, 1293.
Li, X.F., 2005. Int. J. Solids Struct. 42, 3185.
Li, J.Y., Dunn, M.L., 1998. J. Intell. Mater. Syst. Struct. 7, 404.
Liu, J.X., Liu, X., Zhao, Y., 2001. Int. J. Eng. Sci. 39, 1405.
McMeeking, R.M., 1999. Eng. Fract. Mech. 64, 217.
Nan, C.W., 1994. Phys. Rev. B. 50, 6082.
Qin, Q.H., 2001. Fracture Mechanics of Piezoelectric Materials. WIT Press, Southampton, Boston.
Sih, G.C., Song, Z.F., 2003. Theor. Appl. Fract. Mech. 39, 209.
Spyropoulos, C.P., Sih, G.C., Song, Z.F., 2003. Theor. Appl. Fract. Mech. 39, 281.
Tian, W.Y., Gabbert, U., 2005. Mech. Mater. 37, 565.
Wang, B.L., Mai, Y.-W., 2003. Euro. J. Mech. A/Solids 22, 591.
Wang, B.L., Mai, Y.-W., 2004. Mech. Res. Commun. 31, 65.
Zhang, T.Y., Zhao, M.H., Tong, P., 2002. Adv. Appl. Mech. 38, 147.